

Received 26 November 2022, accepted 5 December 2022, date of publication 12 December 2022,
date of current version 15 December 2022.

Digital Object Identifier 10.1109/ACCESS.2022.3228249

RESEARCH ARTICLE

Dielectric Loss of EPDM Insulation Subjected to Thermal Stress and Pressure

ZHIPENG LEI¹, QINGHUI HE¹, DAVIDE FABIANI², (Senior Member, IEEE), YANG LIU¹,
WEI WANG³, WEI LI¹, YE WANG¹, AND DONGDONG YANG³

¹Shanxi Key Laboratory of Mining Electrical Equipment and Intelligent Control, College of Electrical and Power Engineering, Taiyuan University of Technology, Taiyuan 030024, China

²Department of Electrical, Electronic, and Information Engineering "G. Marconi," University of Bologna, 40136 Bologna, Italy

³State Grid Shanxi Electric Power Research Institute, Taiyuan 030012, China

Corresponding author: Zhipeng Lei (leizhipeng@163.com)

This work was supported in part by the National Natural Science Foundation of China under Grant 51977137; and in part by the Fundamental Research Program of Shanxi Province under Grant 202102040201001, Grant 202103021224115, and Grant 202003D111008.

ABSTRACT The insulation performance of ethylene propylene diene monomers (EPDMs) subjected to multi-stresses in the field is always obscure. To understand the effects of temperature and pressure on the performance of the EPDMs used as insulators for power cables, in this work, focuses were on the dielectric losses of EPDMs under the temperature range of 30–120°C and pressure range of 2–8 bar. The polarization and depolarization currents and the dielectric loss factor of EPDMs under the above conditions have been first measured. The relationship between the depolarization current and dielectric loss factor has been studied based on the correlation of the depolarization charge and the dielectric loss factor at low-frequency. The experimental results showed that the conduction currents and the dielectric loss factor increase with the increase in temperature, but the effect of pressure on the dielectric properties of EPDM is more complicated. There is a strong correlation between the depolarization charge and low-frequency dielectric loss factor, both of which can reflect the change law of the EPDMs' performance. Moreover, the asymmetry coefficient of the dielectric loss factor at low-frequency can be a supplement with regard to describing the deterioration degree of EPDM insulation. The evaluation chart of the insulation performance of the EPDMs has been advanced according to the asymmetry coefficient and the total dielectric loss calculated by the polarization and depolarization currents.

INDEX TERMS Ethylene propylene diene monomer, dielectric loss, polarization current, thermal stress.

I. INTRODUCTION

To achieve net-zero carbon emissions by 2050, it is necessary to reduce the use of fossil energy, such as fuel oil, etc., which derives new energy vehicles such as all-electric aircraft, electric ships, and electric vehicles with rubber wheels, etc [1], [2], [3]. Ethylene propylene diene monomer (EPDM)-insulated cables is key components of the power supply in their hybrid power systems, as they are characterized with excellent moisture resistance, thermal resistance, and oxidation resistance [4], [5], [6]. However, the EPDM-insulated cables in the mining electric vehicle or electrical equipment

are usually subjected to the multi-physics field, i.e. the combined effects of electrical, thermal, and mechanical stresses and other factors, which gradually cause microdefects and further accelerate the deterioration of EPDMs [7], [8], [9]. In a degradation process, the destruction of molecular chains affects the internal carrier concentration and mobility, resulting in changes in the performance of cables.

Scholars have accumulated some experimental and research results with regard to the challenges of evaluating the performance of EPDM-insulated cables in the field. Burnay, Calmeta, Ohiki, and Fabiani et al. focused on the research of EPDM insulation performance under electrical stress, thermal stress, and irradiation. Based on the mechanical, physical, and chemical properties of EPDMs when affected

The associate editor coordinating the review of this manuscript and approving it for publication was Zhouyang Ren¹.

by temperature under different irradiation conditions, they concluded that the change in free radicals, such as hydrocarbons or the carbon groups formed by the fracture defects of the main bonds, is the main reason for the performance deterioration of EPDMs [10], [11], [12], [13]. Men studied the space charge characteristics and physicochemical properties of EPDMs under thermal stress and found that molecular chain breaks increase the number of polar groups and ions. Moreover, the complex changes in the physical and chemical structures during thermal ageing resulted in a change in the insulation performance [14]. Cao studied the ethylene propylene rubber insulation under high electrical stress and thermal stress and calculated the time-to-failure data of a 63.2% breakdown probability based on the two-parameter Weibull distribution. The calculation result was fitted into Crine's model [15]. Zhou designed a bending-thermal combined ageing test platform, he concluded that mechanical bending has an accelerating effect on the deterioration of the EPR insulation layer [16]. The above-mentioned studies are significant for understanding the performance of the EPDM insulations subject to multi-stresses. Moreover, it is commonly accepted that the failures of cable insulation result from the combined effects of multi-stresses and that the superposition of individual stress effects is not equivalent to the effect caused by combined stresses [17], [18]. Therefore, to further understand the insulation performance of the EPDM cables under multi-stresses, e.g., electrical, thermal, and mechanical stresses, in this work, the main focus was on studying the dielectric loss of EPDM under different temperatures and pressures according to different methods.

In this paper, an EPDM insulation for flexible rubber-sheathed cables designed for mining electrical equipment was taken as a research object. The polarization and depolarization currents (PDCs) and the dielectric loss factor of the EPDM under different temperatures and pressures were measured, and the correlation between the depolarization charge quantity and low-frequency dielectric loss was studied. Moreover, the characteristic describing the deteriorating degree of the EPDM insulation was calculated, including the conductance loss and polarization loss. The method of evaluating the insulation performance of EPDM was given by the dielectric loss of the PDCs at low-frequency and their asymmetry coefficient.

II. EXPERIMENTAL DESCRIPTIONS

A. SAMPLE PREPARATION

In this paper, a DCJ30M ethylene propylene rubber film was used to make samples. This refined and filtered film, conforming to the requirements of GB 7594.8-1987 rubber insulation and rubber sheath of electric cables and wires part 8: rubber sheath 90°C, can be directly used in insulating the flexible cables used in coal mining. Before the preparation, the surface of the mold and films was cleaned with anhydrous alcohol, and the unvulcanized film was preheated at 120°C for 2 min. The film was first vulcanized for

15 min under 160°C and 14 MPa. Then, the sample and mold were naturally cooled down to room temperature. Finally, cured samples wiped with alumina foil were pretreated for 24 h in a vacuum drying oven at 80°C to eliminate the by-products and mechanical stress. The thickness of the samples was 0.5–0.6 mm.

B. POLARIZATION AND DEPOLARIZATION CURRENT MEASUREMENT

Fig. 1 shows the diagram of the measurement system of the PDCs, where the three-electrode structure is used to avoid the surface current effect. KEYSIGHT B2981A was selected as an ammeter. Since PDC is sensitive to external interference, the sample and electrodes were placed in an enclosed stainless steel cylinder connected to the ground for shielding. The cylinder was placed in an oven controlling the sample's temperature. The PDC of the sample was measured under different pressures and temperatures. The pressures were approximately 2 bar, 4 bar, 6 bar, and 8 bar, and they were controlled by different weights. The temperatures were approximately 30°C, 60°C, 90°C, and 120°C. Approximately 30 min after the pressure and temperature reached the set values, the PDC was measured.

At the beginning of the measurement, to avoid damaging the high charging current to the ammeter, the switch S_2 was closed to short-circuit the ammeter before the constant positive DC voltage was applied to the sample. Afterwards, after ~ 5 s, the voltage was applied, the switch S_2 was opened, and the ammeter started to measure the polarization current, $i_p(t)$, for more than 600 s. The field strength during the polarization is 1 kV/mm. Before the measurement of the depolarization current, the switch S_2 was closed again. Just thereafter, the DC source was removed, and the switch S_1 was connected to position 2 to short-circuit the HV electrode to the ground. Less than 5 s later, the switch S_2 was reopened, and the depolarization current, $i_{dp}(t)$, was measured for more than 600 s.

The steady-state conductance current of EPDM was measured by the same PDC measurement system. The field strength is 1 kV/mm, 3 kV/mm, 5 kV/mm, 10 kV/mm, 15 kV/mm, and 25 kV/mm. Before the polarization current test, the sample was discharged for 600 s.

C. DIELECTRIC LOSS FACTOR MEASUREMENT

Fig. 2 shows a schematic diagram of the dielectric loss factor measurement system. The sample was clamped between the upper and lower electrodes, which are connected to the broadband dielectric impedance spectroscopy, NOVOCONTROL Concept 80, by two 50- Ω coaxial cables. The sample was placed in an oven, which acts as the temperature controller and the shielding chamber. The setting value and applying method of pressure and temperature were the same as those of the PDC measurement procedure. The measuring voltage was 3 V rms, and the frequency range was 0.01–10⁵ Hz.

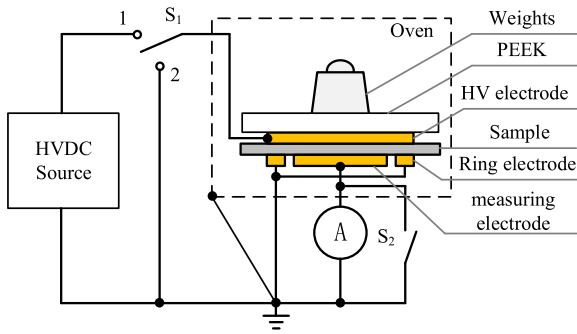


FIGURE 1. Schematic diagram of the PDC measurement system.

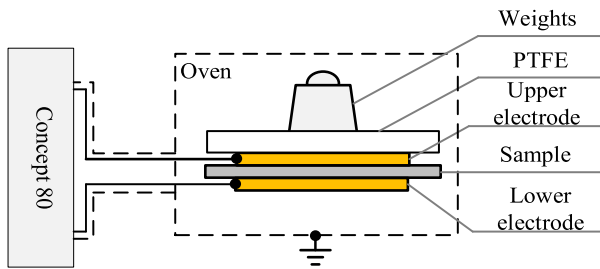


FIGURE 2. Diagram of the dielectric loss factor measurement system.

Generally, the thickness of EPDMs slightly decreases with the increase in pressure. For example, when the pressure is 8 bar, the thickness decreases by ~13%. To avoid the thickness change effect on the measuring results, the used thicknesses of the samples were the thicknesses after pressure was applied for ~30 min at the measuring temperature. To further ensure the consistency of the errors, the same samples were measured using the PDC and dielectric loss factor measurement systems with the same temperature and different pressures. Before each measurement, the samples were discharged for more than 12 h at 80°C.

III. MEASURING RESULTS

A. PDC OF EPDM

Fig. 3 shows the PDC of the EPDM at different temperatures when a constant pressure of 6 bar and an electric field of 1 kV/mm were applied. The depolarization current was taken as the absolute value. According to the figures, both the polarization current, $i_p(t)$, and depolarization current, $i_{dp}(t)$, of the EPDMs decreased with time, t . Affected by the dielectric polarization, PDC rapidly decreased at the initial measurement stage. The downward trend of PDC became slower and finally tended to have a stable value. At the same pressure, the PDC of the EPDM under a low field (1 kV/mm) increased with the increase in temperature. Namely, the higher the measurement temperature, the higher the current amplitude at the same time.

The change in the carriers' mobility in the sample is the main reason for the increase in the polarization current under different temperatures. The quasi-steady-state conductance current density J_s was calculated according to the steady-state

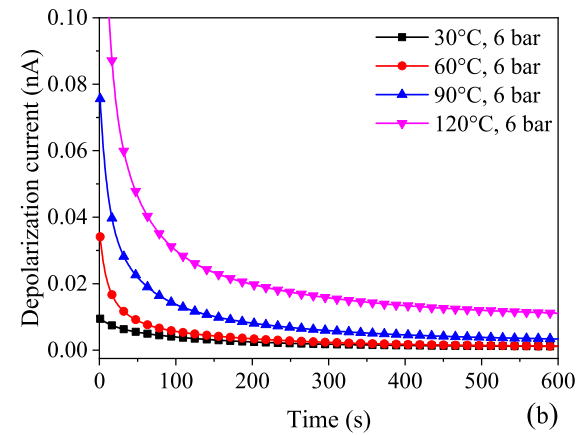
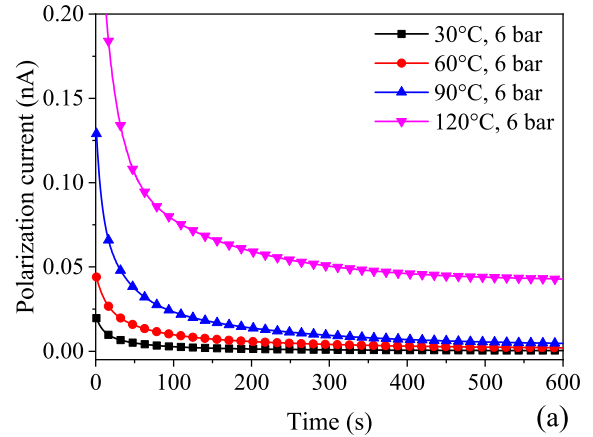


FIGURE 3. PDC of EPDM at different temperatures: (a) polarization current and (b) depolarization current.

conductance current i_∞ of the polarization current as follow:

$$J_s = \frac{i_\infty(t)}{A_{mel}} \quad (1)$$

where $i_\infty(t)$ is the steady-state conductance current value at 600 s; A_{mel} is the area of the measurement electrode.

Based on the relationship of the quasi-steady-state conductance current density J_s with the electric field strength E , the threshold field strength V_Ω was obtained as shown in Table 1, which is the electric field strength in the intersection of the Ohm's law with the space charge limit current theory in $\lg J_s - \lg E$. So the carrier mobility μ_f at the threshold field strength V_Ω was calculated by

$$\mu_f = \frac{8j_\Omega d^3}{9V_\Omega^2 \epsilon_f \epsilon_0} \quad (2)$$

Fig. 4 shows the dependency of the carriers' mobility on the temperature at different pressures. It can be seen that the carrier mobility exponentially increases with the increase in temperature. In this case, the electrical conductivity of EPDM increases with the increase in temperature, leading to an increase in the polarization current. According to the theory of the thermally stimulated current [19], [20], the depth of the charge trap is deepened with the increase in temperature.

TABLE 1. Threshold field strength at different temperatures and pressures.

Parameter	$T(^{\circ}\text{C})$	2 bar	4 bar	6 bar	8 bar
V_{Ω} (kV/mm)	30	10.085	10.256	9.846	9.713
	60	9.730	10.064	9.439	9.406
	90	9.497	9.791	9.307	9.126
	120	9.487	9.760	9.291	8.996

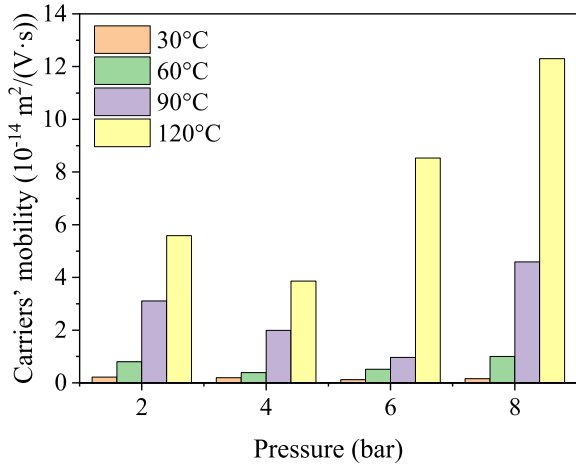


FIGURE 4. Carrier mobility of EPDM at different temperatures.

Heat promotes the detrapping of charges in deeper traps during depolarization processes, resulting in an increase in the depolarization current.

Fig. 5 shows the PDC of EPDM at different pressures when a temperature of 90°C and an electric field of 1 kV/mm were applied. As shown in Fig. 5(a), the polarization current first decreased and then increased with the increase in pressure. Under a pressure of 6 bar, the steady-state current, *i. e.*, the conduction current, decreased to minimum, ~5 pA. When the pressure increased to 8 bar, the conduction current reached ~24 pA, which is obviously higher than the current at other pressures. The difference in the depolarization current is slight. When the pressure was ~4 bar or 6 bar, the descending rate of the depolarization current was higher during the first 300 s. However, the quasi-steady-state current at different pressures was almost the same.

The increase in pressure causes the tight alignment of the molecular chains [21], weakening the polarization process. Meanwhile, a decrease in free volume [22] weakens the migration process of ion-equivalent carriers.

B. DIELECTRIC LOSS FACTOR OF EPDM

Fig. 6 shows the dielectric loss factor, $\tan\delta$, at different temperatures when the pressure was 2 bar, 4 bar, 6 bar, and 8 bar, respectively. It can be seen that at a frequency lower than ~10 Hz, the dielectric loss factor always increased with the increase in temperature. This phenomenon generally results

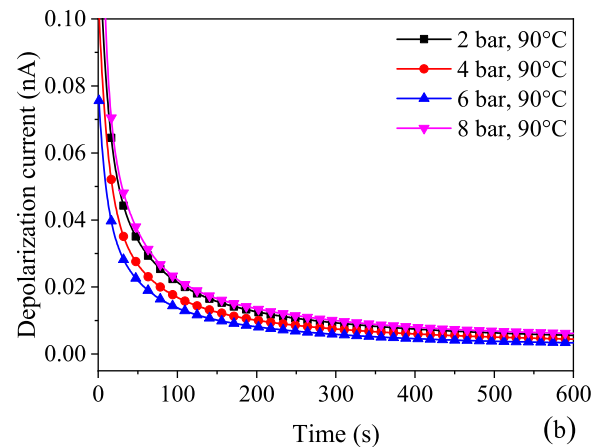
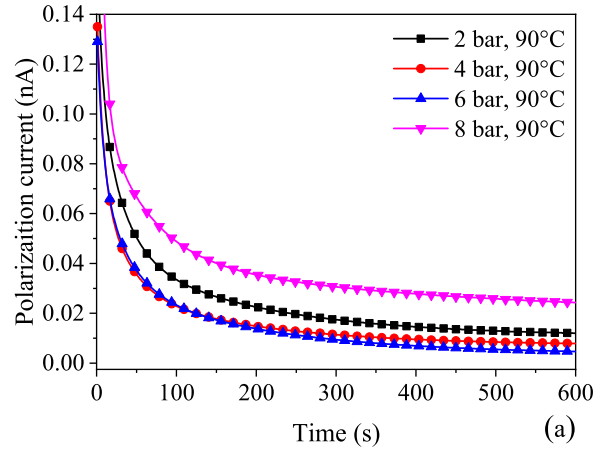


FIGURE 5. PDC of EPDM at different pressures: (a) polarization current and (b) depolarization current.

from the polarization of electrodes, depending on the sample conductivity. For example, the conduction current of EPDM at 120°C was ~43 pA higher than that at other temperatures, as shown in Fig. 3(a). Under this condition, the charges from the thermal activation have enough time to migrate from one side of EPDM to the other side under the influence of the electric field, causing increases in the leakage current and dielectric loss factor.

The pressure effect on the dielectric loss factor of EPDM is more complicated. Fig. 7 shows the dielectric loss factor at the frequency of 0.01 Hz. It can be seen that the dielectric loss factor was almost constant at temperatures of 30°C and 60°C. When the temperature increased to 90°C, the dielectric loss factor decreased with the increase in pressure. However, the dielectric loss factor at 120°C showed an evidently reverse trend, as it increased from ~0.9 to ~1.4. This phenomenon results from the effect of temperature and pressure on the polarization and conduction of EPDM. When the temperature is no more than ~90°C, the motion of molecular chains is limited by the increase in pressure, which weakens the polarization and conduction process of EPDM. When the temperature reaches ~120°C, the molecular thermal motion

plays a dominant role, the bonds between the molecules weaken, and carrier concentration shows an evident growth, which results in the increase of the dielectric loss factor.

At the low frequency, the trend of the dielectric loss factor with pressure is different at different temperatures, which refers to the conductivity and Maxwell/Wagner/Sillars polarization. As shown in Fig. 8, with the temperature rising, the conductivity of EPDM increases. However, because of the nonlinear relationship of conductivity with pressure, the rising rate of conductivity at different temperatures is different.

Considering the effect of conductivity, the dielectric loss factor can be expressed as

$$\tan \delta(\omega) \approx \frac{\frac{\sigma_0}{\varepsilon_0 \omega^s} + \frac{(\varepsilon_s - \varepsilon_\infty)\omega\tau}{1 + \omega^2\tau^2}}{\varepsilon_\infty + \frac{(\varepsilon_s - \varepsilon_\infty)\omega\tau}{1 + \omega^2\tau^2}} \quad (3)$$

where σ_0 is conductivity; ε_0 is the dielectric permittivity of vacuum; $0 < s \leq 1$; ε_s and ε_∞ are the limiting values of the real part of complex permittivity ε' when $\varepsilon' \rightarrow 0$ and $\varepsilon' \rightarrow \infty$, respectively.

According to (3) and Fig. 8, the trend of the dielectric loss factor, which should be similar to the trend of conductivity, increases with the temperature rising. The rising rate of the dielectric loss factor decreases firstly, then increases with the pressure rising. Obviously, only considering the effect of conductivity can not explain the trend of the dielectric loss factor. When the temperature rises, the Maxwell/Wagner/Sillars polarization takes part. For analyzing the effect of the Maxwell/Wagner/Sillars polarization, the complex electric modulus was introduced to suppress the influence of conductivity.

As shown in Fig. 9, the dielectric dispersion regions can be observed at the lower frequency domain. The relaxation phenomena at the lower frequency are ascribed to the interfacial polarization or Maxwell/Wagner/Sillars polarization [23], which are generally taken into consideration during the investigation of an inhomogeneous medium. Due to the contaminants and heterogeneous dispersion in EPDM samples after the vulcanization, the build-up of charges at the interface between different various phases can lead to the interfacial polarization of EPDM medium [24]. The value of the dielectric loss factor was obtained near the relaxation peak which leads to a different trend. For example, at 90°C, the dielectric loss factor of 0.01 Hz at different pressures lies in the decline area of the relaxation; at 120°C, the dielectric loss factor of 0.01 Hz is the rising area of the relaxation. In conclusion, due to the conductivity and Maxwell/Wagner/Sillars polarization, the dielectric loss factor at different temperatures shows a different trend with pressure.

IV. DISCUSSION

A. RELATIONSHIP BETWEEN THE DEPolarization CURRENT AND DIELECTRIC LOSS FACTOR

Based on the results of the experiment, the conduction and polarization currents can represent the change in the

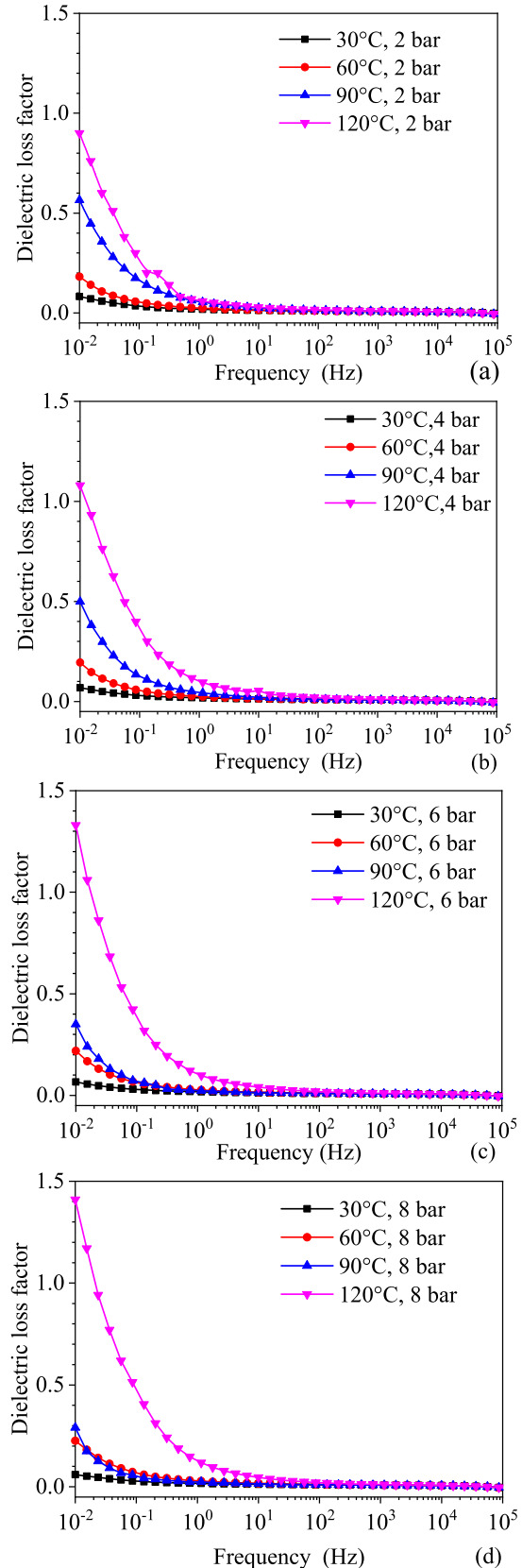


FIGURE 6. Dielectric loss factor of EPDM at different temperatures when the pressure is (a) 2 bar, (b) 4 bar, (c) 6 bar, and (d) 8 bar.

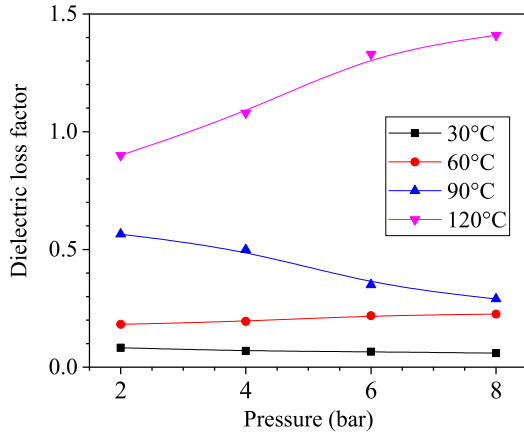


FIGURE 7. Dielectric loss factor of EPDM at different temperatures.

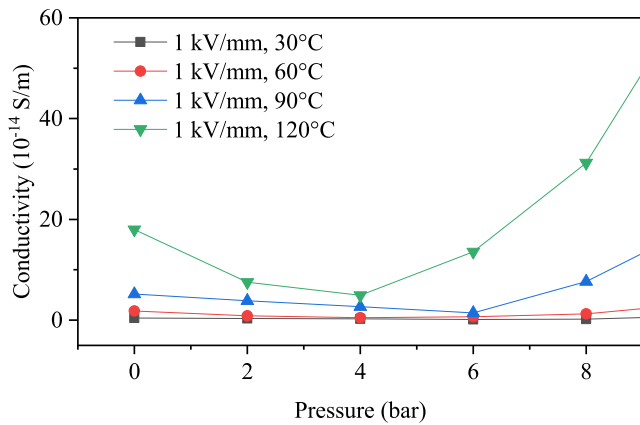


FIGURE 8. Conductivity of EPDM at different pressures and temperatures.

insulation performance of EPDM under various pressure and temperature values. With the increase in temperature, the insulation performance of EPDM is degraded, and the depolarization current and dielectric loss factor decrease. For further analyzing the performance of EPDM, the depolarization charge quantity and the dielectric loss factor at 0.1 Hz are exacted as typical characteristics. The depolarization charge quantity, Q_{dp} , which is a typical characteristic value describing the insulation state and is calculated by the depolarization current [25], can be expressed as follows:

$$Q_{dp} = \int_1^{600} i_{dp} dt \quad (4)$$

Fig. 10 shows the correlation between the depolarization charge quantity and low-frequency dielectric loss factor of EPDM under different pressures and temperatures. It can be seen that both the depolarization charge quantity and low-frequency dielectric loss factor increase with the increase in temperature and that they are related to the applied pressure. The higher the pressure, the quicker the growing rate of the two characteristics with the increase in temperature.

To further clarify the correlation between the depolarization charge quantity and dielectric loss factor at 0.1 Hz, the

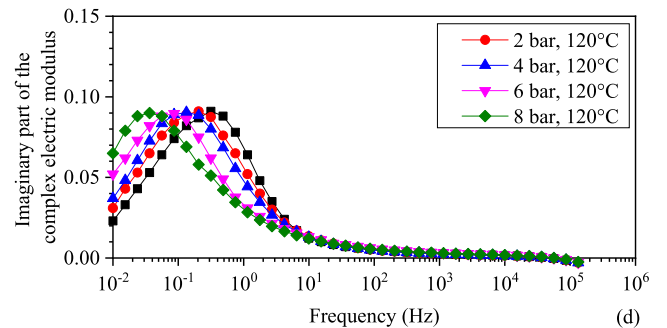
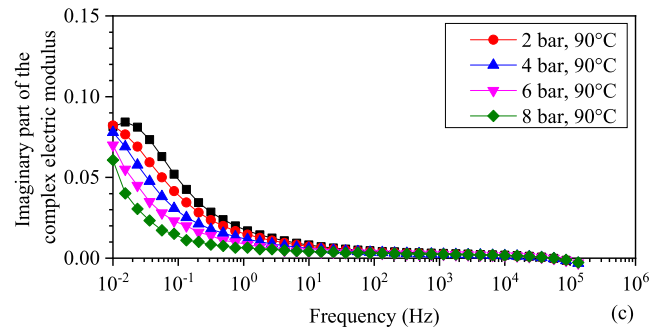
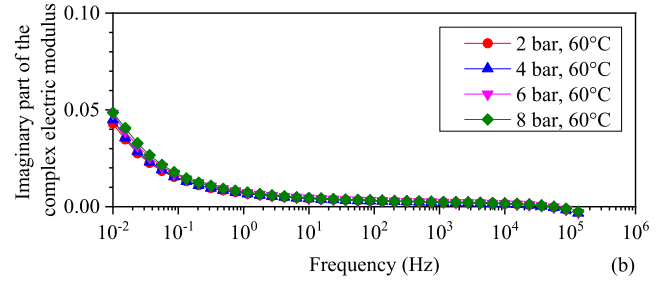
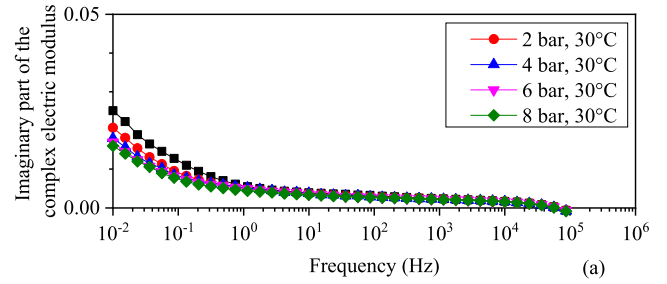


FIGURE 9. Imaginary part of the complex electric modulus when the temperature is (a) 30°C, (b) 60°C, (c) 90°C, and (d) 120°C.

Pearson correlation coefficient method was used to analyze the relevance. Supposing that two characteristics, x and y , are obtained by several experiments, denoted as x_i and y_i ($i = 1, 2, \dots, n$), then the mathematical expression of the correlation coefficient, r , is as follows:

$$r = \frac{\sum_{i=1}^n (x_i - \bar{x})(y_i - \bar{y})}{\sqrt{\sum_{i=1}^n (x_i - \bar{x})^2 \sum_{i=1}^n (y_i - \bar{y})^2}} \quad (5)$$

where \bar{x} and \bar{y} are the average values of x_i and y_i , respectively. The correlation coefficient is between -1 and $+1$, which is the absolute value $|r| \leq 1$. The closer $|r|$ is to 1, the higher the linear correlation between x and y is. In general, the degree

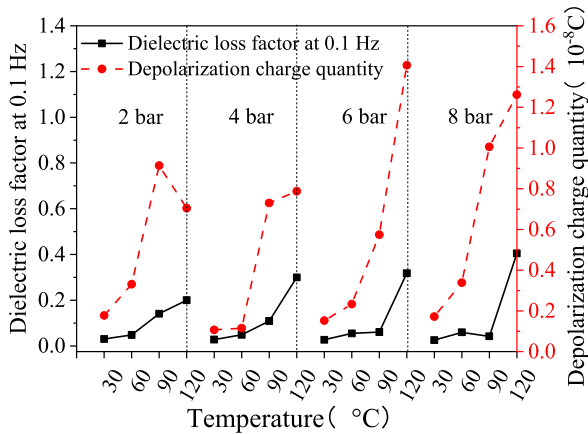


FIGURE 10. Correlation between the charge quantity of the depolarization current and low-frequency dielectric loss factor.

TABLE 2. Correlation coefficient of the depolarization charge quantity and low-frequency dielectric loss factor.

Pressure (bar)	2	4	6	8
<i>r</i>	0.841	0.812	0.969	0.731

of correlation can be divided into the following cases: $|r| \geq 0.8$ represents high correlation; $0.5 \leq |r| < 0.8$ represents moderate correlation; $0.3 \leq |r| < 0.5$ represents low correlation; and $|r| < 0.3$ shows that the relevance between the two characteristics is very weak, which can be regarded as nonlinear correlation. The correlation coefficient between the depolarization charge quantity and low-frequency dielectric loss factor is shown in Table 2. When the pressure was 2–6 bar, they were highly correlated. When the pressure increased to 8 bar, the correlation coefficient decreased to 0.731, which signifies moderate correlation. Therefore, there is a high correlation between the depolarization charge quantity and the low-frequency dielectric loss factor. Both of them can reflect the change law of EPDM’s performance, which is affected by temperature and pressure.

B. RELATIONSHIP BETWEEN THE DIELECTRIC LOSS AND INSULATION PERFORMANCE

Assuming that the dielectric response function, $f(t)$, of insulating dielectrics, which is proportional to the polarization current or depolarization current, obeys the “Curie-von Schweidler” law, Fourier transform can be performed to convert the dielectric response function from the time domain to the frequency domain [26]. The total loss factor of EPDM in the frequency domain is [27], [28], and [29]

$$\begin{aligned} \tan \delta(\omega) &= \frac{\varepsilon''(\omega)}{\varepsilon'(\omega)} = \frac{\gamma/\varepsilon_0\omega + \chi''(\omega)}{\varepsilon_\infty + \chi'(\omega)} \\ &= \frac{\gamma/\varepsilon_0\omega}{\varepsilon_\infty + \chi'(\omega)} + \frac{\chi''(\omega)}{\varepsilon_\infty + \chi'(\omega)} \\ &= \tan \delta'(\omega) + \tan \delta''(\omega) \end{aligned} \tag{6}$$

where ω is the angular frequency; $\varepsilon'(\omega)$ is the real part of the dielectric permittivity; $\varepsilon''(\omega)$ is the imaginary part of the dielectric permittivity; ε_0 is the vacuum dielectric constant, 8.854×10^{-12} F/m; ε_∞ is the high-frequency component of the dielectric permittivity of EPDM; $\tan \delta'(\omega)$ is the conduction loss; $\tan \delta''(\omega)$ is the polarization loss; and $\chi'(\omega)$ and $\chi''(\omega)$ are the real and imaginary parts of the polarization susceptibility, respectively, namely the real and imaginary parts after the Fourier transform of the dielectric response function. The conductivity, γ , of EPDM under a certain electric field, E , can be obtained as follows:

$$\gamma = J_S/E \tag{7}$$

When the DC conductance compared with the dielectric response function is very low in the polarization current, the dielectric loss factor of EPDM in the frequency domain can be obtained by the Fourier transform of the polarization current. The curves of the dielectric loss from conduction, polarization, and the total dielectric loss with frequency are shown in Fig. 11 to 13, and they were drawn in accordance with the PDCs at different temperatures when the pressure was 6 bar according to (6).

The total dielectric loss of EPDM was higher at low-frequency, and it decreased with the increase in frequency. This is mainly because the carrier moves slowly at low-frequency. Carriers are locally accumulated at the interface between the sample and electrode, forming additional polarization. In addition, an interface was formed between the nonuniform vulcanization area and the uniform vulcanization area in the EPDM. Under the action of the electric field, charges were accumulated in the interface area, and a dipole was generated, forming interface polarization. At low-frequency, the dipole inside the EPDM insulation could overcome the intermolecular force, keep up with the alternating frequency of the electric field, complete the polarization process, and form the polarization loss. Under the influences of conduction and polarization, the total dielectric loss was high in the low-frequency region.

To effectively and accurately describe this asymmetry and discover its changing trend under pressure and thermal stress, the asymmetry coefficient of the dielectric loss at low-frequency was introduced to quantify the degree of asymmetry, which can be defined as follows:

$$K = \frac{\tan \delta(\text{depolarization @ 1kV/mm, 0.1 Hz})}{\tan \delta(\text{polarization @ 1kV/mm, 0.1 Hz})} \tag{8}$$

According to GB/T 12972.1-2008, the $\tan \delta$ of the flexible rubber cables with screens for a rated voltage of 3.6/6 kV should not be higher than 0.035 at 3.6 kV. At this threshold, the insulation is good when $\tan \delta < 0.035$, slightly deteriorated when $0.035 < \tan \delta < 0.1$, and significantly deteriorated when $\tan \delta > 0.1$.

Fig. 14 shows the evaluation chart of the EPDM samples based on the asymmetry coefficient of the dielectric loss at 0.1 Hz. When $\tan \delta$ is lower than 0.035, the insulation state should be good. However, the total dielectric loss of

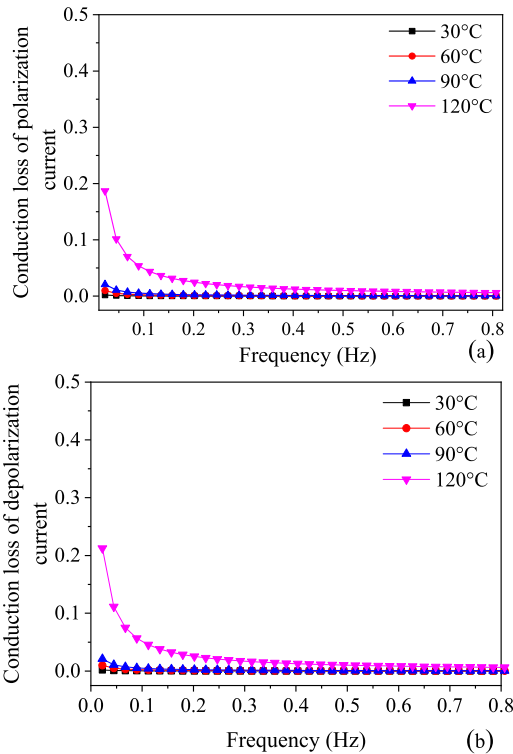


FIGURE 11. Conduction losses of (a) Polarization current and (b) Depolarization current.

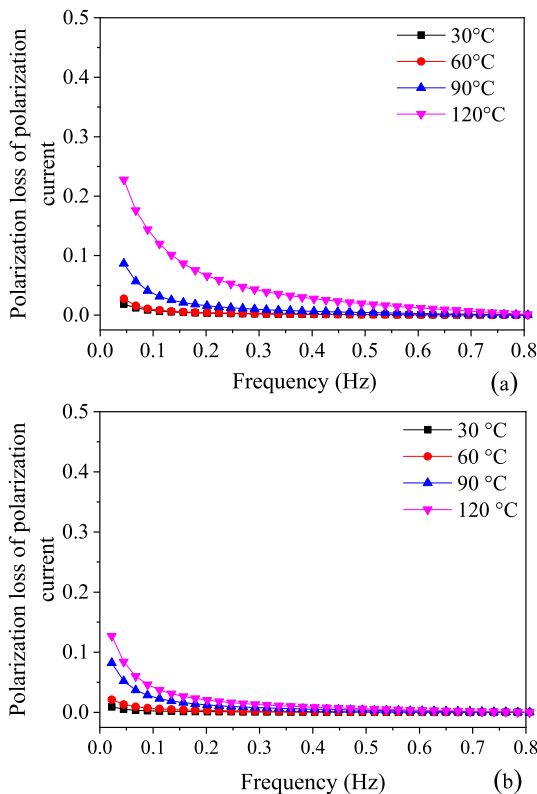


FIGURE 12. Polarization losses of (a) Polarization current and (b) Depolarization current.

polarization and the depolarization current of some samples showed obvious asymmetry under multi-stresses. The

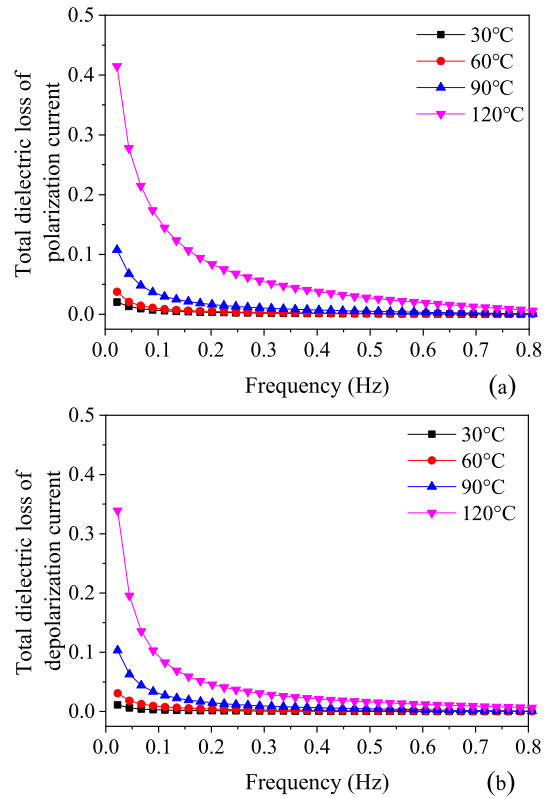


FIGURE 13. Total dielectric losses of (a) Polarization current and (b) Depolarization current.

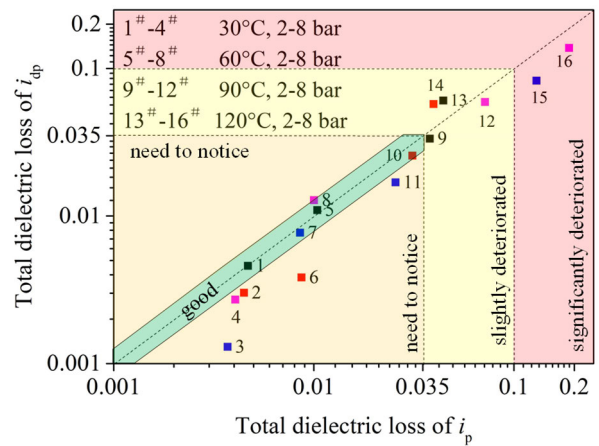


FIGURE 14. Evaluation chart of the insulation performance of EPDM.

asymmetry coefficient, K , showed a weak relevance to pressure. This phenomenon is consistent with the influence of pressure on the dielectric loss factor in Section III. Therefore, it can be considered that when $\tan\delta < 0.035$ and $K \approx 1$, it is preferentially inferred that the EPDM insulation is good. When K is unequal to 1, it is considered that the insulation begins to deteriorate. More attention should be paid to the regular testing of the dielectric loss of insulation. When $\tan\delta$ is higher than 0.035, the asymmetric coefficient has a weak relevance to the degree of the insulation deterioration, and

the asymmetric coefficient can be ignored. The insulation slightly deteriorates when $0.035 < \tan\delta < 0.1$, and the deterioration is serious when $\tan\delta > 0.1$.

It should be noted that with the increase in temperature, the conduction loss increases faster than the polarization loss. In this condition, the total dielectric loss presenting the polarization current also increases faster than the total dielectric loss presenting the depolarization current. Thus, the asymmetry coefficient of the dielectric loss decreases. This is the reason why the asymmetric coefficient of the dielectric loss at low-frequency shows a weak relevance to the degree of insulation deterioration at high temperature.

V. CONCLUSION

In this work, the PDCs and the dielectric loss factor of EPDM insulation were measured under different temperatures and pressures. The depolarization charge quantity and low-frequency dielectric loss factor were used to describe the deteriorating degree of EPDM insulation, and the following conclusions were obtained.

The higher the temperature, the higher the PDCs of EPDM. However, the polarization current of an EPDM subjected to low pressure is lower than that of an EPDM under normal conditions. When the pressure exceeds a certain threshold, ~ 6 bar, the polarization current shows a rising trend with the increase in pressure.

When the frequency is lower than ~ 10 Hz, the dielectric loss factor always increases with the temperature rise. However, the pressure influence on dielectric loss is irregular.

The depolarization charge quantity and low-frequency dielectric loss factor increase with temperature rise, the increasing rate of which shows growth with pressure. Therefore, there is a strong relevance between the depolarization charge quantity and dielectric loss factor at low-frequency. The asymmetry coefficient of the dielectric loss at low-frequency can be a supplement to describe the deterioration degree of EPDM insulation. For good EPDM insulation, $\tan\delta$ should be lower than 0.035 and K should be ~ 1 .

REFERENCES

- [1] C. Li et al., "Insulating materials for realising carbon neutrality: Opportunities, remaining issues and challenges," *High Voltage*, vol. 7, no. 4, pp. 610–632, Aug. 2022, doi: [10.1049/hve2.12232](https://doi.org/10.1049/hve2.12232).
- [2] Z. Shi, C. Li, Z. Lei, Y. Yang, J. He, and J. Song, "Lichtenberg figures presenting electrostatic discharge patterns at different humidity," *J. Phys. D: Appl. Phys.*, vol. 54, no. 34, pp. 1–5, Jun. 2021, doi: [10.1088/1361-6463/AC073D](https://doi.org/10.1088/1361-6463/AC073D).
- [3] Z. Lei, J. Song, M. Tian, X. Cui, C. Li, and M. Wen, "Partial discharges of cavities in ethylene propylene rubber insulation," *IEEE Trans. Dielectr. Electr. Insul.*, vol. 21, no. 4, pp. 1647–1659, Aug. 2014, doi: [10.1109/TDEI.2014.004297](https://doi.org/10.1109/TDEI.2014.004297).
- [4] L. Lin, C. Lin, P. Geng, Z. Lei, J. Song, and M. Tian, "Aging life evaluation of coal mining flexible EPR cables under multi-stresses," *IEEE Access*, vol. 8, pp. 53539–53546, 2020, doi: [10.1109/ACCESS.2020.2981359](https://doi.org/10.1109/ACCESS.2020.2981359).
- [5] T. L. Hanley, R. P. Burford, R. J. Fleming, and K. W. Barber, "A general review of polymeric insulation for use in HVDC cables," *IEEE Elect. Insul. Mag.*, vol. 19, no. 1, pp. 13–24, Jan. 2003, doi: [10.1109/MEI.2003.1178104](https://doi.org/10.1109/MEI.2003.1178104).
- [6] G. Zuidema, W. Kegerise, R. Fleming, M. Welker, and S. Boggs, "A short history of rubber cables," *IEEE Elect. Insul. Mag.*, vol. 27, no. 4, pp. 45–50, Jul. 2011, doi: [10.1109/MEI.2011.5954068](https://doi.org/10.1109/MEI.2011.5954068).
- [7] C. Xu, R. Zhao, C. Li, Y. Li, G. Zhang, T. Shahsavarian, M. Yuan, and Z. Lei, "Significant enhancement in the electrical conductance properties of ethylene propylene diene monomer using the nano-SiO₂ particles," *High Voltage*, vol. 6, no. 3, pp. 487–494, Mar. 2021, doi: [10.1049/HVE2.12070](https://doi.org/10.1049/HVE2.12070).
- [8] R. Men, Z. Lei, T. Han, D. Fabiani, C. Li, S. V. Suraci, and J. Wang, "Effect of long-term fluorination on surface electrical performance of ethylene propylene rubber," *High Voltage*, vol. 4, no. 4, pp. 339–344, Dec. 2019, doi: [10.1049/HVE.2019.0005](https://doi.org/10.1049/HVE.2019.0005).
- [9] S. V. Suraci and D. Fabiani, "Aging modeling of low-voltage cables subjected to radio-chemical aging," *IEEE Access*, vol. 9, pp. 83569–83578, 2021, doi: [10.1109/ACCESS.2021.3086987](https://doi.org/10.1109/ACCESS.2021.3086987).
- [10] S. G. Burnay, "An overview of polymer ageing studies in the nuclear power industry," *Nucl. Instrum. Methods Phys. Res. B, Beam Interact. Mater. At.*, vol. 185, nos. 1–4, pp. 4–7, Dec. 2001, doi: [10.1016/S0168-583X\(01\)00757-1](https://doi.org/10.1016/S0168-583X(01)00757-1).
- [11] J. F. Calmet, F. Carlin, T. M. Nguyen, S. Bousquet, and P. Quinot, "Irradiation ageing of CSPE/EPR control command electric cables. Correlation between mechanical properties and oxidation," *Radiat. Phys. Chem.*, vol. 63, nos. 3–6, pp. 235–239, Mar. 2002, doi: [10.1016/S0969-806X\(01\)00585-0](https://doi.org/10.1016/S0969-806X(01)00585-0).
- [12] D. Fabiani and S. V. Suraci, "Broadband dielectric spectroscopy: A viable technique for aging assessment of low-voltage cable insulation used in nuclear power plants," *Polymers*, vol. 13, no. 4, p. 494, Feb. 2021, doi: [10.3390/POLYM13040494](https://doi.org/10.3390/POLYM13040494).
- [13] S. Hanada, M. Miyamoto, N. Hirai, L. Yang, and Y. Ohki, "Experimental investigation of the degradation mechanism of silicone rubber exposed to heat and gamma rays," *High Voltage*, vol. 2, no. 2, pp. 92–101, May 2017, doi: [10.1049/HVE.2017.0009](https://doi.org/10.1049/HVE.2017.0009).
- [14] R. Men, Z. Lei, J. Song, Y. Li, L. Lin, M. Tian, D. Fabiani, and X. Xu, "Effect of thermal ageing on space charge in ethylene propylene rubber at DC voltage," *IEEE Trans. Dielectr. Electr. Insul.*, vol. 26, no. 3, pp. 792–800, Jun. 2019, doi: [10.1109/TDEI.2018.007752](https://doi.org/10.1109/TDEI.2018.007752).
- [15] L. Cao and S. Grzybowski, "Aging phenomenon of 15 kV EPR cable insulation by electrical and thermal stress," in *Proc. Int. Conf. High Voltage Eng. Appl.*, Shanghai, China, Sep. 2012, pp. 480–483.
- [16] L. Zhou, C. Liu, S. Quan, X. Zhang, and D. Wang, "Experimental study on ageing characteristics of electric locomotive ethylene propylene rubber cable under mechanical–thermal combined action," *High Voltage*, vol. 7, no. 4, pp. 792–801, Mar. 2022, doi: [10.1049/HVE2.12202](https://doi.org/10.1049/HVE2.12202).
- [17] G. Mazzanti, "The combination of electro-thermal stress, load cycling and thermal transients and its effects on the life of high voltage ac cables," *IEEE Trans. Dielectr. Electr. Insul.*, vol. 16, no. 4, pp. 1168–1179, Aug. 2009, doi: [10.1109/TDEI.2009.5211872](https://doi.org/10.1109/TDEI.2009.5211872).
- [18] A. C. Gjerde, "Multifactor ageing models—Origin and similarities," *IEEE Elect. Insul. Mag.*, vol. 13, no. 1, pp. 6–13, Jan./Feb. 1997, doi: [10.1109/57.567392](https://doi.org/10.1109/57.567392).
- [19] G. Li, X. Liang, J. Zhang, X. Li, Y. Wei, C. Hao, Q. Lei, and S. Li, "Insulation properties and interface defect simulation of distribution network cable accessories under moisture condition," *IEEE Trans. Dielectr. Electr. Insul.*, vol. 29, no. 2, pp. 403–411, Apr. 2022, doi: [10.1109/TDEI.2022.3157902](https://doi.org/10.1109/TDEI.2022.3157902).
- [20] Y. Wei, J. Yang, G. Li, X. Zhou, C. Hao, Q. Lei, and S. Li, "Influence of molecular chain side group on the electrical properties of silicone rubber and mechanism analysis," *IEEE Trans. Dielectr. Electr. Insul.*, vol. 29, no. 4, pp. 1465–1473, Aug. 2022, doi: [10.1109/TDEI.2022.3175443](https://doi.org/10.1109/TDEI.2022.3175443).
- [21] S. Li, W. Wang, S. Yu, and H. Sun, "Influence of hydrostatic pressure on dielectric properties of polyethylene/aluminum oxide nanocomposites," *IEEE Trans. Dielectr. Electr. Insul.*, vol. 21, no. 2, pp. 519–528, Apr. 2014, doi: [10.1109/TDEI.2013.004131](https://doi.org/10.1109/TDEI.2013.004131).
- [22] Y. Wang, Y. Yang, and M. Tao, "Understanding free volume characteristics of ethylene-propylene-diene monomer (EPDM) through molecular dynamics simulations," *Materials*, vol. 12, no. 4, pp. 1–18, Feb. 2019, doi: [10.3390/ma12040612](https://doi.org/10.3390/ma12040612).
- [23] G. C. Psarras, K. G. Gatos, P. K. Karahaliou, S. N. Georga, C. A. Krontiras, and J. Karger-Kocsis, "Relaxation phenomena in rubber/layered silicate nanocomposites," *Exp. Polym. Lett.*, vol. 1, no. 12, pp. 837–845, 2007, doi: [10.3144/expresspolymlett.2007.116](https://doi.org/10.3144/expresspolymlett.2007.116).
- [24] Z. Lei, J. Song, P. Geng, M. Tian, L. Lin, C. Xu, C. Feng, J. Zeng, and Z. Li, "Influence of temperature on dielectric properties of EPR and partial discharge behavior of spherical cavity in EPR insulation," *IEEE Trans. Dielectr. Electr. Insul.*, vol. 22, no. 6, pp. 3488–3497, Dec. 2015, doi: [10.1109/TDEI.2015.004942](https://doi.org/10.1109/TDEI.2015.004942).

- [25] M. Dakka, A. Bulinski, and S. Bamji, "On-site diagnostics of medium-voltage underground cross-linked polyethylene cables," *IEEE Elect. Insul. Mag.*, vol. 27, no. 4, pp. 34–44, Jul. 2011, doi: 10.1109/MEI.2011.5954067.
- [26] M. Farahani, H. Borsi, and E. Gockenbach, "Dielectric response studies on insulating system of high voltage rotating machines," *IEEE Trans. Dielectr. Electr. Insul.*, vol. 13, no. 2, pp. 383–393, Apr. 2006, doi: 10.1109/TDEI.2006.1624283.
- [27] A. A. Shayegani, E. Gockenbach, H. Borsi, and H. Mohseni, "Investigation on the transformation of time domain spectroscopy data to frequency domain data for impregnated pressboard to reduce measurement time," *Electr. Eng.*, vol. 89, no. 1, pp. 11–20, Oct. 2006, doi: 10.1007/S00202-005-0316-0.
- [28] W. S. Zaengl, "Dielectric spectroscopy in time and frequency domain for HV power equipment. I. Theoretical considerations," *IEEE Electr. Insul. Mag.*, vol. 19, no. 5, pp. 5–19, Oct. 2003, doi: 10.1109/MEI.2003.1238713.
- [29] K. Zhou, H. Yuan, Y. Li, M. Li, Z. Li, and S. Lin, "Assessing aging status and type of XLPE cable insulation with a graphic approach based on PDC measurement," *IEEE Trans. Power Del.*, vol. 37, no. 6, pp. 5114–5123, Dec. 2022, doi: 10.1109/TPWRD.2022.3170947.



ZHIPENG LEI received the M.Sc. and Ph.D. degrees from the Taiyuan University of Technology, in 2010 and 2015, respectively.

He was a Visiting Scholar with the Department of Electrical Electronics and Information Engineering, University of Bologna, in 2018. He is currently an Associate Professor at the College of Electrical and Power Engineering, Taiyuan University of Technology. His research interests include the condition assessment of high-voltage

cable failure and associated partial discharges characteristics, space charge properties of insulation, and intelligence techniques in coal mine.



QINGHUI HE received the B.Sc. degree from Shijiazhuang Tiedao University, China, in 2018. She is currently pursuing the M.Sc. degree with the College of Electrical and Power Engineering, Taiyuan University of Technology, Taiyuan, China. Her research interests include high voltage and insulation technology.



DAVIDE FABIANI (Senior Member, IEEE) received the M.Sc. and Ph.D. degrees (Hons.) in electrical engineering, in 1997 and 2002, respectively. He is currently an Associate Professor in innovative electrical technologies and design and diagnostics of electrical insulation at the Department of Electrical Electronics and Information Engineering, University of Bologna. His research interests include development, characterization, and diagnosis of electrical insulation systems for

applications in electrical and electronic apparatus. He is the coauthor of about 220 papers, most of them published on the major international journals and conference proceedings. He is an Associate Editor of *IET High Voltage* and the Vice President for Technical Activities of IEEE DEIS (2020–2021).



YANG LIU received the B.Sc. and M.Sc. degrees from the Taiyuan University of Technology, China, in 2017 and 2021, respectively.



WEI WANG received the B.Sc. and M.Sc. degrees from the Taiyuan University of Technology, China, in 2012 and 2015, respectively. His research interests include high voltage and insulation technology.



WEI LI received the B.Sc. degree from the Hefei University of Technology, China, in 2019. He is currently pursuing the M.Sc. degree with the College of Electrical and Power Engineering, Taiyuan University of Technology, Taiyuan, China. His research interests include high voltage and insulation technology.



YE WANG received the B.Sc. degree from Shanxi University, China, in 2018, and the M.Sc. degree from the Taiyuan University of Technology, China, in 2021.



DONGDONG YANG received the B.Sc. degree from the Taiyuan University of Technology, Taiyuan, China, in 2006, and the M.Sc. degree from the Nanjing University of Aeronautics and Astronautics, China, in 2009. He is currently an Electrical Engineer and works with the Shanxi Electrical Research Institute. His research interests include equipment insulation detection technology and the power distribution Internet of Things technology.

...